ISSN 1063-7788, Physics of Atomic Nuclei, 2023, Vol. 86, No. 3, pp. 238–245. © Pleiades Publishing, Ltd., 2023.
Russian Text © The Author(s), 2023, published in Yadernaya Fizika, 2023, Vol. 86, No. 3, pp. 388–395.

ELEMENTARY PARTICLES AND FIELDS
Experiment

Measurement of the $e^+e^- \to n\bar{n}$ Cross Section near the Threshold with a High Energy Resolution

A. V. Bobrov[1),2)*] and A. E. Bondar[1),2)]**

Received October 30, 2022; revised November 30, 2022; accepted December 21, 2022

Abstract—A method for measuring cross sections at e^+e^- colliders for the case where the center-of-mass frame of colliding particles moves in the laboratory frame is proposed. Within this method, the energy dependence of the cross section is extracted from the angular distribution of interaction products. The method applied to the $e^+e^- \to n\bar{n}$ process is found to be sensitive. This method provides the possibility of studying the fine structure of the cross section near the threshold at scales much less than the energy spread of the beams used. Similar measurements may be implemented in experiments at the Super Charm-Tau Factory.

DOI: 10.1134/S1063778823030043

1. INTRODUCTION

The direct-counting method is the main tool for measuring cross sections at electron–positron colliders. The integrated luminosity reached in an experiment is measured by employing processes characterized by large cross sections and described by quantum electrodynamics, such as $e^+e^- \to e^+e^-$ and $e^+e^- \to \gamma\gamma$. The cross section for the process being studied is determined using the number of detected events minus the background and the integrated luminosity at each point in energy. In this traditional approach, the resolution with respect to structures that are narrow or change rapidly with energy is determined by the beam-energy spread. The existing e^+e^- colliders have a high degree of monochromaticity—$\dfrac{\delta E_b}{E_b} \sim 10^{-3}$, where E_b is the beam energy. If the cross section σ as a function of the invariant mass W of product particles ($W \simeq 2E_b$) changes rapidly with respect to the invariant-mass spread δ_W $\left(\delta_W \simeq \sqrt{2}\delta E_b\right)$—that is, $\dfrac{d\sigma}{\sigma dW} \gg \dfrac{1}{\delta_W}$—then it is difficult or is impossible to study the energy dependence of the cross section. The proposed method makes it possible to overcome these difficulties.

If the center-of-mass (c.m.) frame moves in the laboratory frame, the emission angle of a heavy product particle with respect to the direction of motion of the c.m. frame is related to the momentum and, hence, to the kinetic energy of this particle in the c.m. frame. Measurement of the angular distribution of heavy product particles in the laboratory frame permits substantially improving the energy resolution in measuring the energy dependence of the cross section for the production of a pair of heavy particles. Within the method considered in the present study, it is assumed that, for some reasons, the momentum of a heavy product particle cannot be measured—for example, in the case of the production of a $n\bar{n}$ pair or a $p\bar{p}$ pair in which the energy of protons is insufficient for traversing the accelerator vacuum chamber, so that one can measure only the emission direction by the antiparticle-annihilation point in the detector.

The motion of the c.m. frame is provided by the application of the Crab Waist scheme [1]. Within this approach, the arrangement of the collision point is changed in such a way that the beams intersect at a relatively large angle in the horizontal plane. For example, this angle is equal to 82 mrad in the case of the Super KEKB factory. If the energies of colliding beams are equal to each other, the c.m. frame moves in the laboratory frame along the bisector of the collision angle almost orthogonally to the direction of primary-beam motion.[3)] The velocity of the c.m.

[1)]Budker Institute of Nuclear Physics, Siberian Branch, Russian Academy of Sciences, Novosibirsk, Russia.
[2)]Novosibirsk State University, Novosibirsk, Russia.
*E-mail: A.V.Bobrov@inp.nsk.su
**E-mail: A.E.Bondar@inp.nsk.su

[3)]At the present time, two similar Super Charm-Tau Factory projects are considered in China [2, 3] and Novosibirsk [4]. Either makes it possible to implement the proposed scheme of measurement of the $e^+e^- \to N\bar{N}$ cross section at the threshold.

frame is equal to the sine of half the collision angle in units of the speed of light. The inaccuracy in measuring the average energies of the beams and their energy spread is an important parameter. In order to measure the cross section at scales much less than δ_W, the absolute inaccuracy in measuring these quantities should be much less than δ_W. The inverse Compton scattering method applied at the existing colliders has an inaccuracy of about 100 keV (at the $n\bar{n}$ production threshold) and satisfies this criterion [5].

The experimental data existing at the present time are indicative of an interesting behavior of the cross section for the production of a baryon–antibaryon pair ($N\bar{N}$) near the threshold in e^+e^- annihilation. It is likely that, owing to final-state baryon interaction, the cross section grows fast in the immediate vicinity of the threshold [6–9]. Possibly, the characteristic scale at which the cross section changes is substantially smaller than δ_W. In order to test theoretical predictions made in [10–13], it is necessary to reduce the inaccuracy of experimental measurements of the energy dependence of the cross sections—in particular, at energy scales substantially smaller than the beam-energy spread.

The present study is devoted to exploring the resolution of the method and the possible limitations on its accuracy by means of a numerical simulation.

2. DESCRIPTION OF THE METHOD

Let us consider the proposed method by applying it to the process $e^+e^- \to n\bar{n}$ at colliding-beam energies near the threshold for neutron–antineutron pair production. Near the threshold (even with allowance for the fact that the c.m. frame moves in the laboratory frame at a speed much lower than the speed of light), the probability for neutron detection is much lower than the probability for the detection of the antineutron, which can be detected with a high efficiency by its annihilation in the calorimeter. On the basis of the coordinates of the cluster center in the calorimeter and the beam-collision point, the antineutron emission angle can be measured to a rather high degree of precision. The position of the beam-collision point is known to a high precision since the beams collide at a large angle, so that the size of the luminosity region is substantially reduced.

In the case of a fixed invariant mass W of the product pair (less than the critical value of $W^\star = m_n\left(2+v^2\right)$), the maximum antineutron-emission angle $\alpha_{\max}$ with respect to the direction of the velocity of the c.m. frame is bounded and is related to W by the simple equation (obtained in the nonrelativistic approximation)

$$\alpha_{\max} = \sqrt{\frac{W-2m_n}{m_n v^2}}, \qquad (1)$$

where m_n is the neutron mass and v is the velocity of the c.m. frame. As was indicated above $v = \sin\gamma$, where γ is half of the beam-collision angle. Assuming that the distribution of the antineutron emission angle in the c.m. frame is known, one can obtain the distribution of events with respect to the emission angle in the laboratory frame for angles between 0 and $\alpha_{\max}$. The total angular distribution can be obtained by summing the angular distributions for all energy intervals with a weight that is equal to the integrated luminosity multiplied by the cross section for a given energy interval. The exact expressions for the critical angle of the distributions at a fixed invariant mass are presented in the Appendix. Within the proposed method, the energy dependence of the cross section is extracted statistically over the whole ensemble of events, in just the same way as in the direct-counting method, but, in each individual event, the invariant mass of the product pair is not determined.

A fast-simulation code was used to study the process of reconstruction of the $e^+e^- \to n\bar{n}$ cross section on the basis of the angular distribution. The energies and angles of initial particles in beams were generated with allowance for the following assumptions. The energy of beam particles obeys a normal distribution with a relative spread of $\delta E_b/E_b = 10^{-3}$. The angular spread in the beam is 10^{-3} rad. The angular distribution of antineutrons in the c.m. frame corresponds to the S-wave production.[4)] Half of the beam-collision angle was chosen to be $\gamma = 0.05$. The production of neutron–antineutron pairs was simulated at ten points in beam energy over the interval of [939.75; 942.0] MeV with a step of 0.25 MeV. The energy of 940.74 MeV corresponds to the threshold for $n\bar{n}$ pair production. The energy dependence of cross section for the production of a neutron–antineutron pair was described either by a Heaviside Θ function having a step at the production threshold (the cross section value is 1 nb) or by a monotonically growing cross section with an additional contribution or one or two hypothetical resonances at the threshold. The resonance widths were assumed to be 100 keV.

In order to obtain the cross section, simulated events are broken down into statistically independent sets. One group of the data is used to determine the shape of the angular distributions as a function of the invariant mass W. After that, the resulting angular distributions are used to describe the distributions of the other part of the data, which plays the role of "experimental" data. The cross sections are measured

[4)] This seems quite justified since the method is applicable in a narrow energy range above the production threshold. A substantial contribution of the D wave will manifest itself in the ϕ asymmetry with respect to the direction of motion of the c.m. frame in the laboratory frame.

several times for independent sets of "experimental" data. The accuracy of these measurements is determined from the root-mean-square deviation of their results.

The invariant-mass distribution of events, $\frac{dN}{dW}$, is determined by minimizing the distributions $\frac{d^2N}{dn_y dn_z}$ and $\frac{d^2N}{d\cos\alpha dE_b}$. Here, n_i are the projections of the direction of antineutron motion (vector $\frac{\mathbf{p}}{|\mathbf{p}|}$, where $\mathbf{p}$ is the antineutron 3-momentum vector) onto the respective axes (the c.m. frame moves along the x axis) and α is the angle between the velocities of the neutron and c.m. frame. The approximating function depends linearly on the sought parameters of $\frac{dN}{dW}$. The cross section is determined by the formula $\sigma(W) = \frac{dN}{dW}/\frac{d\mathcal{L}}{dW}$ (here, $\mathcal{L}$ is the integrated luminosity). The luminosity distribution as a function of the invariant mass $\frac{d\mathcal{L}}{dW}$ is assumed to be known. In experiments, it is calculated on the basis of the beam energies and energy spread.

3. INVARIANT-MASS RESOLUTION

As has already been indicated, there is no direct functional relation between the antineutron emission angle and the invariant mass of the $n\bar{n}$ pair. If we express the difference $W - 2m_n$ in terms of the maximum scattering angle α, there arises the relation

$$W - 2m_n = m_n v^2 \sin\alpha.$$

This relation was obtained in the approximation where the deviations of the 4-momentum of the pair of product nucleons, δP_i, from the P_i value calculated on the basis of the average values of the 4-momenta of primary particles have only a parallel component $\delta P_{i||}$ (see Appendix). The presence of a nonzero orthogonal component $\delta P_{i\perp}$ leads to errors in measuring the angle α. At the threshold, $\alpha = 0$; therefore, an expansion in the small parameter $\delta\alpha$ to second-order terms inclusive should be used in the error-transfer formula

$$\frac{\delta W}{m_n} = v^2\sqrt{4\alpha^2(\delta\alpha)^2 + (\delta\alpha)^4}. \qquad (2)$$

It is noteworthy that the term containing the first derivative leads to a relatively fast deterioration of the resolution. Indeed, the first- and second-order contributions become commensurate as soon as the critical angles reach values about the angular resolution.

We will now obtain a numerical estimate of the invariant-mass resolution on the basis of this formula. For this, we consider the following basic factors contributing to the invariant-mass resolution:

- Inaccuracy in measuring the antineutron-emission angle;
- Energy spread of particles in beams;
- Radiative corrections;
- Inaccuracy in measuring beam energies and energy spread in beams.

The characteristic transverse size of the electromagnetic-calorimeter crystal is about 5 cm. The distance from the collision point (for particles emitted in the direction of the velocity of the c.m. frame) is about one meter. Under the assumption that the antineutron-annihilation point in the electromagnetic calorimeter can be determined with a precision of one crystal, the angular resolution is about 1/20 rad. After the substitution into (2), the relative invariant-mass resolution turns out to be about 10^{-5}. Antineutron scattering in the detector material before the interaction in the calorimeter may additionally impair the angular resolution with respect to the antineutron-emission direction, but, according to estimates, this did not make a substantial contribution in the invariant-mass resolution.

Because of the energy spread, the direction of the velocity of motion of the c.m. frame and its magnitude change from one event to another. The characteristic angular spread is $\delta\alpha = \frac{\delta E_b}{\sqrt{2}E_b v}$. The substitution into Eq. (2) accordingly leads to a quadratic dependence of the invariant-mass resolution on the relative energy spread at the production threshold:

$$\frac{\delta W}{m_n} = \frac{(\delta E_b)^2}{2E_b^2} \sim 10^{-6}. \qquad (3)$$

In the case of measurement of the cross section for the production of heavy particles near the threshold, the effect of radiative corrections is suppressed for two reasons. First, final-state radiation of slow heavy particles is weak. Second, the energy of photons emitted by primary electrons is bounded by the difference of the e^+e^- energy and the energy threshold for the production of heavy particles and is about the beam-energy spread. Therefore, the effect of radiative corrections on the inaccuracy of cross section measurements is on the same order of magnitude as the effect of the energy spread.

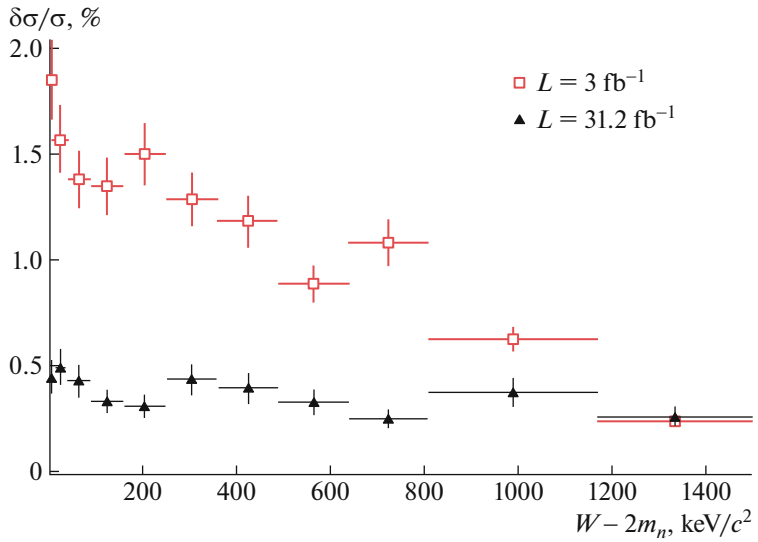

Fig. 1. Relative inaccuracy of cross section measurements as a function of the invariant mass at various values of the integrated luminosity. The horizontal bars show the bin width. The binning used is specified in Table 1. The beam energy is 940.75 MeV.

4. SYSTEMATIC UNCERTAINTIES IN CROSS SECTION MEASUREMENTS

The main problem restricting the accuracy in measuring the production cross section for neutron–antineutron pairs consists in determining the efficiency of antineutron detection in the detector used. The currently existing codes for calculating antineutron interaction with matter at low energies give no way to determine reliably either the antineutron-annihilation probability or the detector response in that case. A calibration of the detector by means of tagged antineutrons in the process $e^+e^- \to \Lambda^0\bar{\Lambda}^0 \to p\pi^- + \bar{n}\pi^0$ remains the only reliable means for determining the detection efficiency.

Moreover, the presumed inaccuracy in measurements of the beam energies and energy spread by the inverse Compton scattering method is about 100 keV or $10^{-4}E_b$ [5], as was indicated above, and has but a slight effect on the invariant-mass resolution. However, a simulation revealed that the errors in measuring the energies and especially the energy spread contribute to the inaccuracy of the cross section measurement. At the inaccuracy of 10% (the respective absolute inaccuracy is 130 keV) in the energy-spread measurement, the relative systematic shifts in the cross section reaches 10%. This effect can be partly reduced by optimizing the distribution of the integrated luminosity with respect to the invariant mass (here, we imply the mean invariant mass calculated with equilibrium parameters of primary particles). In the case of accumulation at a fixed point in energy, the distribution function $\frac{d\mathcal{L}}{dW}$ has a Gaussian form $\frac{\mathcal{L}_{\rm exp}(-(W-W_0)^2/(2\delta_W^2))}{\sqrt{2\pi}\delta_W}$, where W_0 is the mean value of the invariant mass. Here, we do not discriminate between the invariant masses of initial, e^+e^-, and, final, $n\bar{n}$, particles, disregarding radiative corrections. If the distribution function $\frac{d\mathcal{L}}{dW_0}$ is uniform, the resulting distribution $\frac{d\mathcal{L}}{dW}$ obtained after the convolution with the Gaussian distribution will also be uniform. Within this scenario of integrated-luminosity accumulation, the contribution of the inaccuracy in measurements of the energies and energy spread to the error in the cross section is suppressed since $\frac{d\mathcal{L}}{dW}$ is independent of the beam energies and energy spread.

5. RESULTS

On the basis of the results of simulations, it was found that the sensitivity is rather high, provided that the invariant mass of the product pair is less than the critical energy, $W < m_n(2+v^2) = W^\star$. Otherwise, the invariant-mass resolution becomes several-fold lower in a jump-like way. For the implementation of a high-resolution mode, the number of events in

Table 1. Size of bins in invariant mass for constant cross section

Bin	1	2	3	4	5	6	7	8	9	10	11
$W - 2m_n$, keV	10	40	90	160	250	360	490	640	810	1170	∞

Table 2. Partition of bins in invariant mass for hypothetical resonances

Bin	1	2	3	4	5	6	7	8	9	10
$W-2m_n$, keV	40	80	120	160	200	240	280	320	360	400
Bin	11	12	13	14	15	16	17	18	19	20
$W-2m_n$, keV	440	480	520	560	600	640	3680	720	760	800
Bin	21	22	23	24	25	26	27	28	29	30
$W-2m_n$, MeV	0.96	1.12	1.28	1.44	1.60	1.76	1.92	2.08	2.24	2.4
Bin	31	32	33	34	35	36	37	38	39	40
$W-2m_n$, MeV	3.34	4.28	5.22	6.16	7.10	8.04	8.98	9.92	10.86	11.80

which $W > W^\star$ should be relatively small. This imposes constraints on the parameter $R = \dfrac{W^\star - 2m_n}{\delta_W}$. If it is small, the high-resolution mode is inaccessible. In our simulation, this parameter is 1.7.

Figure 1 shows the relative inaccuracy in cross section measurement as a function of the invariant mass at various values of the integrated luminosity for the case where, in the simulation, the cross section was taken in the form of the Heaviside Θ step function. In the region extending up to 10 keV, the characteristic resolution is 0.5–0.25% at the integrated luminosity of 31.2 fb^{-1}. The partition into invariant-mass bins is specified in Table 1. It is of interest to compare the inaccuracy obtained here for cross section measurements with the lowest possible inaccuracy of measurements performed at an "ideal" collider (that which has monochromatic beams) by the direct-counting method. At the same integrated luminosity (partitioned into 11 points in energy), the inaccuracy of cross section measurements in an ideal case is about 0.06% at each point. Figures 2 and 3 show the results of the reconstruction of the cross section in the presence of hypothetical resonances. Here, the total integrated luminosity is 70 fb^{-1}. It is distributed uniformly among seven points in energy from $E_b = 940.25$ to $E_b = 941.75$ MeV with a step of 0.25 MeV. It should be noted that resonance structures are not observed in the energy dependence of the cross section obtained by the direct-counting method.

6. CONCLUSIONS

The proposed approach makes it possible to obtain a much higher resolution in the $n\bar{n}$ invariant mass (and, hence, a much higher accuracy of cross section measurements) than that in the case of employing the direct-counting method. This permits studying the structure of cross sections at scales much less than the energy spread. This approach can be generalized to other processes by employing information about the velocity of the reconstructed particle in the laboratory frame.

The statistical inaccuracy of cross section measurements varies in the range of 0.5–0.25% at invariant masses below the critical value $W^\star$ at an integrated luminosity of about 30 fb^{-1} and the cross section of 1 nb for the process being studied. The region where the cross section is measurable to a high precision is determined primarily by the velocity of the c.m. frame and, hence, by the angle of intersection of colliding particles.

The contribution of the angular and energy spread of primary particles in the beam to the inaccuracy of determining the cross section is negligible against the contributions of other factors. Among them, it is necessary to single out the following:

- Inaccuracy in measuring antineutron emission angle;
- Detection efficiency;
- Scattering of antineutrons before their annihilation in the calorimeter;
- Available integrated luminosity and absolute cross section value;
- Absolute inaccuracy in measuring average energies and energy spread in beams;
- Difference of the angular distribution in the c.m. frame from an isotropic distribution;
- Effects of radiative corrections;
- Background conditions.

In order to take accurately into account these effects, it is necessary to perform a complete simulation of the detector, processes induced by antineutron interaction with matter, their reconstruction, and the production of $n\bar{n}$ pairs. However, a qualitative analysis of these effects shows that allowance for them does not change basic conclusions drawn from our present study.

Both Super Charm-Tau Factory projects mentioned above [2–4] envisage the possibility of data accumulation at the threshold for $n\bar{n}$ production with

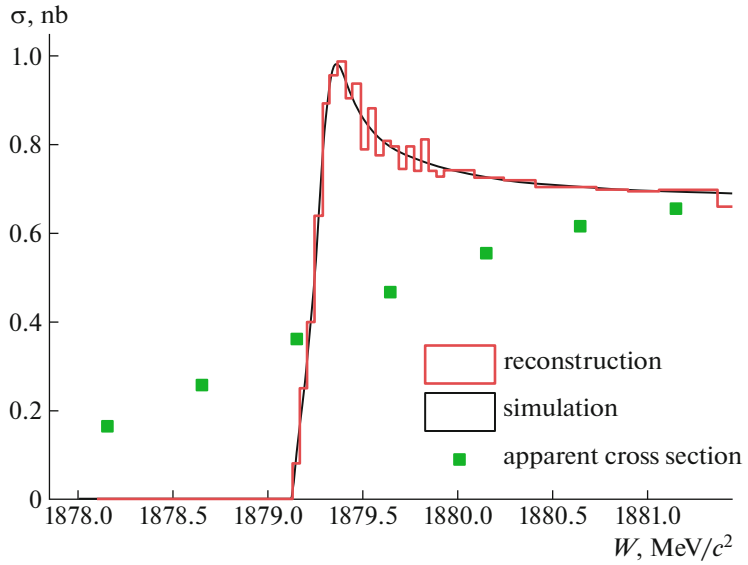

Fig. 2. Reconstruction of the cross section for one hypothetical resonance near the threshold. A fine structure of the cross section is reliably identifiable by the proposed method. The partition into bins in invariant mass is specified in Table 2.

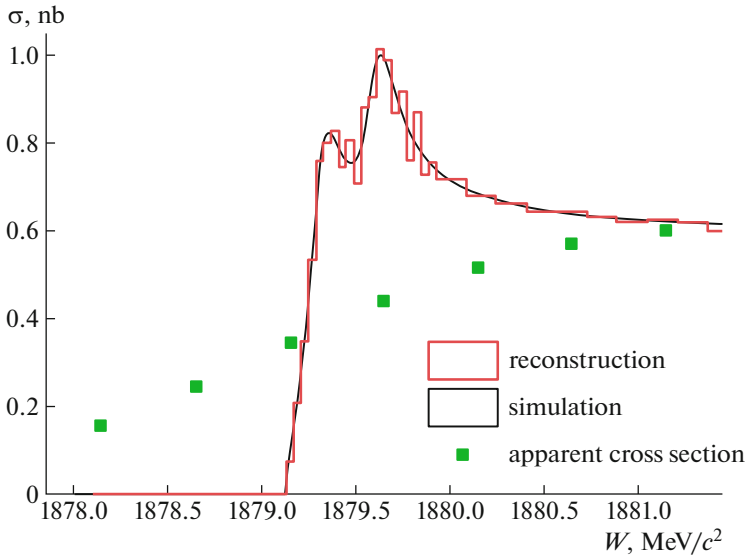

Fig. 3. Reconstruction of the cross section for two hypothetical resonances near the threshold. The apparent cross section changes only slightly upon going over to two resonances, but measurements for the angular distribution show a substantial distinction. The partition into bins in invariant mass is specified in Table 2.

the aim of studying this process. The need for reaching a high luminosity at low energies requires complicating the collider design. In the current state, the luminosity at the threshold for $n\bar{n}$ production is about 10^{34} cm^{-2}s^{-1}. From the above estimates of the inaccuracy in measuring the cross section, it follows that, at an integrated luminosity of 3 fb^{-1} (under the assumption that the cross section for the process being studied is 1 nb), the attainable precision in cross section measurements is 1 to 2%. For the sake of comparison, we indicate that the precision reached by the SND Collaboration in [8] is about 10 to 20% at the resolution scale of about 1 MeV.

Appendix

Let us consider the case of $n\bar{n}$ production under the condition that the $\bar{n}$ emission angle is measurable in the experiment. The angular distribution of $\bar{n}$ in the laboratory frame can be determined from the angular distribution and velocity in the c.m. frame.

We denote by P_i the initial-state 4-momentum calculated without allowance for deviations of the initial-particle 4-momenta from the average values. If δP_i stands for this deviation, it can be decomposed into the components parallel and orthogonal to the initial 4-momentum P_i, $\delta P_i = \delta P_{i||} + \delta P_{i\perp}$. The

perturbation δP_i can be assumed to be small, while $\frac{P_i \delta P_{i||}}{W}$ is the leading term in δW. Neglecting the change in the velocity of the c.m. frame, we discard the term $\frac{\delta P_{i\perp}^2}{2W}$. This is justified from the point of view of perturbation theory.

Let us consider the Lorentz transformation from the c.m. frame to the laboratory frame (we employ the system of units where the speed of light is equal to unity). Instead of two axes orthogonal to the direction of motion of the c.m. frame, we can retain one axis. We denote by T the nucleon kinetic energy in the laboratory frame, by W the invariant mass of the nucleon–antinucleon pair, by m_n the nucleon mass, by v the velocity of the c.m. frame in the laboratory frame, by α the angle between the direction of nucleon motion and the x axis in the laboratory frame (along which the c.m. frame moves), and by ω the scattering angle in the c.m. frame with respect to the velocity of the c.m. frame in the laboratory frame. In the nonrelativistic limit, the transformations in question have the form

$$\begin{bmatrix} 1+v^2/2 & -v & 0 \\ -v & 1+v^2/2 & 0 \\ 0 & 0 & 1 \end{bmatrix} \begin{bmatrix} m_n+T \\ \sqrt{2m_nT}\cos\alpha \\ \sqrt{2m_nT}\sin\alpha \end{bmatrix} = \begin{bmatrix} W/2 \\ \sqrt{W^2/4-m_n^2}\cos\omega \\ \sqrt{W^2/4-m_n^2}\sin\omega \end{bmatrix}.$$

The upper equation is an equation for W:

$$W/2 = \left(1+v^2/2\right)(m_n+T) - v\sqrt{2m_nT}\cos\alpha. \tag{A.1}$$

From Eq. (A.1), we can calculate the nucleon kinetic energy T in the laboratory frame as a function of the antineutron emission angle α and the two-nucleon invariant mass W; that is,

$$T - \frac{v\cos\alpha\sqrt{2m_nT}}{1+v^2/2} + m_n - \frac{W}{2\left(1+v^2/2\right)} = 0.$$

Solving this quadratic equation with respect to $\sqrt{T}$, we obtain

$$\sqrt{T} = \frac{v\cos\alpha\sqrt{2m_n}}{2\left(1+v^2/2\right)} \pm \sqrt{\frac{v^2\cos^2\alpha m_n}{2\left(1+v^2/2\right)^2} - m_n + \frac{W}{2\left(1+v^2/2\right)}}. \tag{A.2}$$

Requiring that the radicand on the right-hand side of Eq. (A.2) be zero, we obtain Eq. (1), which relates the maximum scattering angle to the invariant mass.

Upon employing reasonable input approximations, we can obtain an equation that makes it possible to determine the dependence $\frac{dN}{dW}$ from the distribution $\frac{dN}{d\cos\alpha}$ (we deliberately use $\frac{dN}{dW}$ to emphasize the need for going over to the cross section via $\frac{d\mathcal{L}}{dW}$). The conditions underlying these approximations are the following:

- The angular distribution is not taken into consideration.
- The change in the velocity of the c.m. frame because of the deviations of features of primary particles from the average values is disregarded.
- Events in which the invariant mass exceeds $W^\star$ are rejected.
- The angular distribution of product particles in the c.m. frame is isotropic.
- Radiative corrections are neglected.

In this approximation, the angular distribution in the laboratory frame with respect to the direction of the velocity of the c.m. frame can be represented in the form

$$\frac{d\rho(\cos\alpha,\beta)}{d\cos\alpha} = \begin{cases} \dfrac{\Theta\left(\cos\alpha - \sqrt{1-\sinh^2\beta/\sinh^2\psi}\right)\left(\sinh^2\beta - \sinh^2\psi\sin^2\alpha + \cos^2\alpha\cosh^2\beta\tanh^2\psi\right)}{\cosh^2\psi\sinh\beta\left(1-\cos^2\alpha\tanh^2\psi\right)^2\sqrt{\sinh^2\beta-\sinh^2\psi\sin^2\alpha}}, \\ \text{if} \quad \beta \leqslant \psi, \\ \dfrac{\left(\sqrt{\sinh^2\beta-\sinh^2\psi\sin^2\alpha} + \cos\alpha\cosh\beta\tanh\psi\right)^2}{2\cosh^2\psi\sinh\beta\left(1-\cos^2\alpha\tanh^2\psi\right)^2\sqrt{\sinh^2\beta-\sinh^2\psi\sin^2\alpha}}, \quad \text{if} \quad \beta > \psi. \end{cases} \tag{A.3}$$

REFERENCES

1. P. Raimondi, *Presentation at the 2nd Workshop on SuperB Factory*, LNF-INFN, Frascati, March 2006.
2. Q. Luo and D. Xu, in *Proceedings of the 9th International Particle Accelerator Conference IPAC'2018, Vancouver, Canada, 2018,* p. MOPML013.
3. H.-P. Peng, in *Proceedings of the Charm2018, Novosibirsk, Russia, May 21–25, 2018*.
4. A. Bondar, Phys. At. Nucl. **76**, 1072 (2013).
5. V. E. Blinov, V. V. Kaminsky, E. B. Levichev, N. Yu. Muchnoi, S. A. Nikitin, I. B. Nikolaev, A. G. Shamov, Yu. A. Tikhonov, and V. N. Zhilich, ICFA Beam Dyn. Newslett. **48**, 195 (2009).
6. B. Aubert, R. Barate, D. Boutigny, F. Couderc, Y. Karyotakis, J. P. Lees, V. Poireau, V. Tisserand, A. Zghiche, E. Grauges, A. Palano, M. Pappagallo, A. Pompili, J. C. Chen, N. D. Qi, G. Rong, et al., Phys. Rev. D **73**, 012005 (2006).
7. R. R. Akhmetshin, A. N. Amirkhanov, A. V. Anisenkov, V. M. Aulchenko, V. Sh. Banzarov, N. S. Bashtovoy, D. E. Berkaev, A. E. Bondar, A. V. Bragin, S. I. Eidelman, D. A. Epifanov, L. B. Epshteyn, A. L. Erofeev, G. V. Fedotovich, S. E. Gayazov, A. A. Grebenuk, et al., Phys. Lett. B **759**, 634 (2016).
8. M. N. Achasov, A. Yu. Barnyakov, K. I. Beloborodov, A. V. Berdyugin, D. E. Berkaev, A. G. Bogdanchikov, A. A. Botov, T. V. Dimova, V. P. Druzhinin, V. B. Golubev, L. V. Kardapoltsev, A. S. Kasaev, A. G. Kharlamov, A. N. Kirpotin, I. A. Koop, A. A. Korol, et al., Phys. Rev. D **90**, 112007 (2014).
9. M. Ablikim, M. N. Achasov, P. Adlarson, S. Ahmed, M. Albrecht, R. Aliberti, A. Amoroso, M. R. An, Q. An, X. H. Bai, Y. Bai, O. Bakina, R. Baldini Ferroli, I. Balossino, Y. Ban, K. Begzsuren, et al., arXiv: 2103.12486.
10. V. F. Dmitriev and A. I. Milstein, Phys. Lett. B **658**, 13 (2007).
11. J. Haidenbauer, X.-W. Kang, and U.-G. Meißner, Nucl. Phys. A **929**, 102 (2014).
12. A. I. Milstein and S. G. Salnikov, Nucl. Phys. A **966**, 54 (2017).
13. A. I. Milstein and S. G. Salnikov, Nucl. Phys. A **977**, 60 (2018).